

Shape-independent limits to near-field radiative heat transfer

Owen D. Miller,¹ Steven G. Johnson,¹ and Alejandro W. Rodriguez²

¹*Department of Mathematics, Massachusetts Institute of Technology, Cambridge, MA 02139*

²*Department of Electrical Engineering, Princeton University, Princeton, NJ 08544*

We derive shape-independent limits to the spectral radiative heat-transfer rate between two closely spaced bodies, generalizing the concept of a black body to the case of near-field energy transfer. By conservation of energy, we show that each body of susceptibility χ can emit and absorb radiation at enhanced rates bounded by $|\chi|^2/\text{Im}\chi$, optimally mediated by near-field photon transfer proportional to $1/d^2$ across a separation distance d . Dipole–dipole and dipole–plate structures approach restricted versions of the limit, but common large-area structures do not exhibit the material enhancement factor and thus fall short of the general limit. By contrast, we find that particle arrays interacting in an idealized Born approximation exhibit both enhancement factors, suggesting the possibility of orders-of-magnitude improvement beyond previous designs and the potential for radiative heat transfer to be comparable to conductive heat transfer through air at room temperature, and significantly greater at higher temperatures.

Heat exchange mediated by photons, or radiative heat transfer, can be dramatically modified for bodies separated by small gaps [1–7]. We derive fundamental limits to the near-field spectral heat flux between closely spaced bodies of arbitrary shape, given only their material susceptibilities $\chi(\omega)$ and their separation distance d . The limits feature two enhancements relative to far-field black-body radiative heat transfer: a frequency-dependent “material enhancement factor” $|\chi(\omega)|^2/\text{Im}\chi(\omega)$ that represents resonant enhancement of absorption and emission, and a “near-field enhancement factor” $1/d^2$ arising from large-amplitude evanescent waves. We show that restricted versions of the limit, applied to energy transfer between small particles or between a small particle and a surface, can be approached within a factor of 2. For extended structures, however, common geometries—bulk metals [8–14], thin films [15–21], and elliptical [22–24] or hyperbolic [25–28] metamaterials—fall orders of magnitude short of the limit. We discuss the shortcomings of each geometry, and show that an idealized structure comprising an array of dipolar plasmonic particles, interacting with its mirror image in an additive Born approximation, exhibits both the near-field and material enhancement factors and thus approaches the limit at selected frequencies. This is especially important for applications such as thermophotovoltaics [7, 29–32] where frequency selectivity is crucial.

In ray optics, the scattering properties of a body can be ascribed to its surface. Given the absorptivity of an optical ray at every point along a surface, one has a complete description of the absorptive and emissive properties of the body, leading to the famous black-body limit, and Stefan–Boltzmann law, of thermal radiation [33]. At wavelength and subwavelength scales, the optical physics is very different. Metallic nanoparticles, for example, can absorb and scatter light with effective cross-sections much larger than their physical cross-sections [34], making it difficult even to define quantities like absorptivity. A further difficulty is the presence of near-field evanescent waves, which can increase heat transport beyond the black-body limits, but which do not transmit power in the absence of a reflected evanescent wave [35]. Although the possibility of enhancements beyond

the black-body limit was realized in the 1950s [1, 2], efforts to find underlying limits remain restricted to planar structures (including effective-medium metamaterials) [20, 25, 36–38]. Moreover, heat-transfer calculations have been carried out only in a handful of geometries, including planar bodies with translational symmetry [8–27], simple sphere–sphere [39] and sphere–plate [40–43] configurations and more recently, complex shapes [32, 44–47] that can be studied computationally.

We propose that the quantities limiting near-field heat exchange are the polarization currents within the bodies. Dipoles in vacuum exchange energy at a rate limited by the energy density of an outgoing free-space wave [49] ($\sim 1/r^6$ in the near field, as in van der Waals interactions [50]). We show that optimal energy transfer between material bodies occurs when the currents within the bodies couple individually at the dipole–dipole limit (scaled up by material-resonance enhancements), akin to how ideal ray-optical thermal radiation occurs when a surface has perfect absorptivity. Assuming only the equations of linear (and therefore passive [51]) electromagnetism, we find that the above conditions allow for much greater heat transfer than has previously been shown possible.

In recent work [52] we have shown that conservation of energy imposes fundamental limits to the scattering properties of a metal excited by a fixed incident field. Here, we decompose the heat transfer between two arbitrarily shaped bodies into two separate scattering problems, connected by Lorentz reciprocity [53], ultimately yielding limits that depend only on the product of material enhancements and volume integrals over the background Green’s function. We derive limits for homogeneous, isotropic, and nonmagnetic materials, but the extension to anisotropic, magnetic, and/or chiral materials is straightforward, as discussed below.

Radiative heat exchange is depicted schematically in Fig. 1(a): fluctuating currents arise in body 1 at temperature T_1 , and transfer energy to body 2 by absorption. The net energy transfer from body 1 to body 2 is given by [4]:

$$H_{1\rightarrow 2} = \int_0^\infty \Phi(\omega) [\Theta(\omega, T_1) - \Theta(\omega, T_2)] d\omega, \quad (1)$$

where $\Phi(\omega)$ is the temperature-independent energy flux and

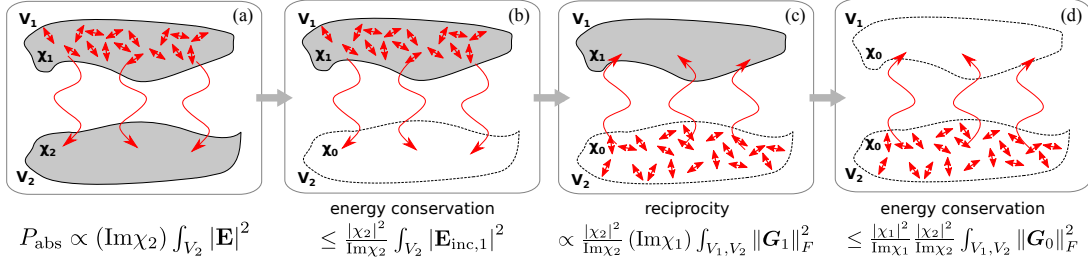


FIG. 1. (a) Radiative heat transfer between two bodies. Energy emanates from fluctuating fields in body 1 (with susceptibility χ_1) and is transferred by absorption to body 2 (with susceptibility χ_2). Limits to the spectral heat flux follow from three steps: (b) Energy conservation bounds the absorption in body 2 in terms of the field incident from body 1, $\mathbf{E}_{\text{inc},1}$, and a resonant enhancement $|\chi|^2/\text{Im}\chi$. (c) Reciprocity (or its modified version [48] for non-reciprocal media) implies that the source and “receiver” locations can be exchanged, whereupon (d) a second scattering problem is again bounded by energy conservation, yielding a limit determined by the material susceptibilities and the free-space GF \mathbf{G}_0 . For near-field transfer the GF integral can be replaced by a term proportional to $1/d^2$, for separation d between the bodies.

Θ is the mean energy per oscillator. $\Phi(\omega)$ is the designable quantity of interest, to be tailored as a function of frequency depending on the application and available materials. We present limits to $\Phi(\omega)$ in the next section.

Limits.—The spectral heat flux $\Phi(\omega)$ can be determined by computing the power absorbed in body 2 (with material susceptibility χ_2) from fluctuating sources in body 1 (with susceptibility χ_1), or vice-versa. In previous work, we have shown how to bound absorption for a fixed incident field [52]: dissipation in a lossy medium must be smaller than the “extinction” (absorption + scattering), which is given by the optical theorem [54–57] and represents the total power extracted from an incident beam. Because absorption is a quadratic functional of the induced currents, whereas extinction is the imaginary part of a linear functional, energy conservation yields limits dependent only on the incident energy and the material susceptibility of the body. A complication in heat transfer is that the sources lie *within* one of the scattering bodies, as in Fig. 1(a), preventing a simple optical theorem.

To circumvent this issue we reframe the scattering problem, without approximation, using a standard integral-equation separation of incident and scattered fields [58]: we define the “incident” field to be the (as-yet unknown) field emanating from the stochastic vector current sources, \mathbf{J} , in the presence of body 1 and the absence of body 2, as in Fig. 1(b), in which case the “scattered” field arises only from the introduction of body 2 (while fully accounting for interactions between bodies 1 and 2). From a volume integral equation (VIE) perspective [58], we define a tensor Green’s function (GF) \mathbf{G}_1 that represents the field of a dipole source in the presence of only body 1, such that the electric field anywhere in space is given by $\mathbf{E} = (i/\epsilon_0\omega) \int_{V_1} \mathbf{G}_1 \mathbf{J} + \chi_2 \int_{V_2} \mathbf{G}_1 \mathbf{E} = \mathbf{E}_{\text{inc},1} + \mathbf{E}_{\text{scat},1}$. This decomposition permits an optical theorem of the usual type, whereby the extinction is proportional to the imaginary part of $\int_{V_2} \mathbf{E}_{\text{inc},1} \cdot \mathbf{E}$, a linear functional of the field induced in body 2. Absorption is given by the usual [54] quadratic functional $\epsilon_0\omega \text{Im}[\chi_2(\omega)] \int_{V_2} |\mathbf{E}|^2/2$. Energy-conservation considerations [52] then yield limits to the power absorbed in

body 2:

$$P_{\text{abs},2} \leq \frac{\epsilon_0\omega}{2} \frac{|\chi_2(\omega)|^2}{\text{Im}\chi_2(\omega)} \int_{V_2} |\mathbf{E}_{\text{inc},1}|^2. \quad (2)$$

As defined above, $\mathbf{E}_{\text{inc},1}$ is given by the convolution of the GF \mathbf{G}_1 with the current sources \mathbf{J} in body 1. From the fluctuation-dissipation theorem [1, 4], the ensemble average of the current–current correlation function can be written as $\langle J_j(\mathbf{x}, \omega), J_k(\mathbf{x}', \omega) \rangle = 4\epsilon_0\omega\Theta(\omega, T_1) \text{Im}[\chi(\omega)] \delta_{jk} \delta(\mathbf{x} - \mathbf{x}')/\pi$. Inserting the currents into Eq. (2) and separating the flux from the Planck spectrum, per Eq. (1), leads to a flux limit

$$\Phi(\omega) \leq \frac{2}{\pi} \frac{|\chi_2(\omega)|^2}{\text{Im}\chi_2(\omega)} \text{Im}[\chi_1(\omega)] \int_{V_1} \int_{V_2} \|\mathbf{G}_1(\mathbf{x}_2, \mathbf{x}_1)\|_F^2 \quad (3)$$

where $\|\cdot\|_F$ denotes the Frobenius norm [59].

The integrand in Eq. (3) represents energy in V_2 due to sources in V_1 , with only body 1 present per Fig. 1(b); by Lorentz reciprocity [53] we can exchange the source and “receiver” locations, i.e. $\mathbf{G}(\mathbf{x}_2, \mathbf{x}_1) = \mathbf{G}^T(\mathbf{x}_1, \mathbf{x}_2)$ as in Fig. 1(c), for any GF in reciprocal media. (The transpose does not affect the norm and can be dropped.) An integral within Eq. (3) represents the power absorbed within body 1, for which the optical theorem applies (because reciprocity moved the sources outside body 1), yielding an energy-conservation [52] bound:

$$\begin{aligned} (\text{Im}\chi_1) \int_{V_1} \|\mathbf{G}_1(\mathbf{x}_2, \mathbf{x}_1)\|_F^2 &= (\text{Im}\chi_1) \int_{V_1} \|\mathbf{G}_1(\mathbf{x}_1, \mathbf{x}_2)\|_F^2 \\ &\leq \frac{|\chi_1|^2}{\text{Im}\chi_1} \int_{V_1} \|\mathbf{G}_0(\mathbf{x}_1, \mathbf{x}_2)\|_F^2 \end{aligned} \quad (4)$$

where \mathbf{G}_0 is the *free-space* GF, as depicted in Fig. 1(d). Inserting Eq. (4) into Eq. (3), the limit to the spectral energy flux between two bodies is

$$\Phi(\omega) \leq \frac{2}{\pi} \frac{|\chi_1(\omega)|^2}{\text{Im}\chi_1(\omega)} \frac{|\chi_2(\omega)|^2}{\text{Im}\chi_2(\omega)} \int_{V_1} \int_{V_2} \|\mathbf{G}_0(\mathbf{x}_1, \mathbf{x}_2)\|_F^2. \quad (5)$$

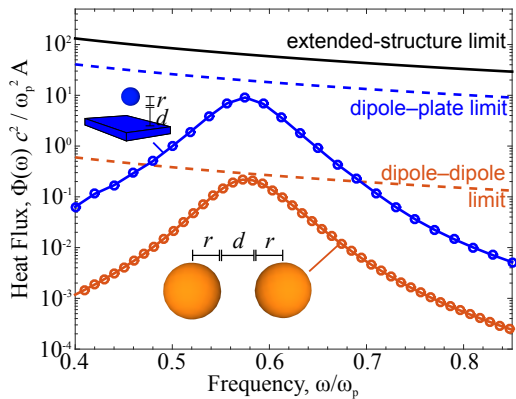


FIG. 2. Comparison of heat flux in sphere–sphere and sphere–plate structures to the analytical limits of Eqs. (8,9). The dipole–dipole limit (dashed red) is approached by two Drude–metal spheres (solid red) at their resonant frequency, $\omega_{\text{res}} \approx \omega_p/\sqrt{3}$. The dipole–plate limit (dashed blue) is approached within a factor of two for a sphere–plate interaction if the material resonance of the plate is slightly modified (see text). In each case the separation distance is $d = 0.1c/\omega_{\text{res}}$, with sphere radii $r = d/5$. The heat transfer exhibits the material enhancement factor $|\chi|^4/(\text{Im } \chi)^2$, but not the near-field enhancement factor, due to the lack of large-area interactions. The area A is taken to be the sphere cross-section πr^2 .

Near-field heat transfer is ideally dominated by the quasistatic term $\mathbf{G}_0 \sim 1/r^3$, which is primarily responsible for the evanescent waves with large surface-parallel wavevectors that enable greater-than-black-body heat-transfer rates [4, 7]. Dropping higher-order terms (further discussed in [SM]), we can bound Eq. (5) by integrating over the infinite half-spaces containing V_1 and V_2 , assuming there is a separating plane between the two bodies. (If not, as e.g. between two curved surfaces, the integrals are similar but with slightly different coefficients.) For bodies separated by a distance d , the integral is given by [SM] $\int_{V_1, V_2} \|\mathbf{G}\|_F^2 = A/32\pi d^2$, where A is the (infinite) area of each half-space. Then the limit to the flux per area is:

$$\frac{\Phi(\omega)}{A} \leq \frac{1}{16\pi^2 d^2} \frac{|\chi_1(\omega)|^2 |\chi_2(\omega)|^2}{\text{Im } \chi_1(\omega) \text{Im } \chi_2(\omega)}. \quad (6)$$

Relative to a black body with $\Phi_{\text{BB}} = k^2 A/4\pi^2$ [4]:

$$\frac{\Phi(\omega)}{\Phi_{\text{BB}}} \leq \frac{1}{4(kd)^2} \frac{|\chi_1(\omega)|^2 |\chi_2(\omega)|^2}{\text{Im } \chi_1(\omega) \text{Im } \chi_2(\omega)}. \quad (7)$$

Eqs. (5–7) provide limits to the near-field spectral heat flux between two bodies and form the central results of this Letter. The $|\chi|^2/\text{Im } \chi$ factors represent resonant absorption/emission enhancements, while the homogeneous GF integral (and ultimately the $1/d^2$ factor) represents limits to the coupling between dipoles in free space [49, 60].

The limits in Eqs. (5–7) can be generalized to a wide class of materials. For anisotropic, magnetic, or chiral materials described by a 6×6 susceptibility tensor $\boldsymbol{\chi}$, each limit generalizes with the replacement $|\chi|^2/\text{Im } \chi \rightarrow \|(\text{Im } \boldsymbol{\xi})^{-1}\|_2$, where

$\boldsymbol{\xi} = -\boldsymbol{\chi}^{-1}$ represents a unitless resistivity [52] and $\|\cdot\|_2$ is the induced matrix 2-norm [59]. This generalization applies even for non-reciprocal media, thanks to a generalized reciprocity theorem [48][SM]. For heat transfer between two bodies in an inhomogeneous background, \mathbf{G}_0 is the background GF.

Dipolar Interactions.—Heat transfer with at least one body approximated as an electric dipole can closely approach the integral-equation limit in Eq. (5). Consider the transfer between two particles of dimensions smaller than their tip-to-tip separation d . For particles with volumes V_i centered at \mathbf{x}_i ($i = 1, 2$), the GF integral in Eq. (5) is approximately $\int_{V_1, V_2} \|\mathbf{G}\|_F^2 = \|\mathbf{G}(\mathbf{x}_1, \mathbf{x}_2)\|_F^2 V_1 V_2$. Defining r_1 and r_2 as the distance between each particle’s tip and center of mass, the limit of Eq. (5) is given by:

$$[\Phi(\omega)]_{\text{dipole-dipole}} \leq \frac{3}{4\pi^3} \frac{|\chi_1(\omega)|^2 |\chi_2(\omega)|^2}{\text{Im } \chi_1(\omega) \text{Im } \chi_2(\omega)} \frac{V_1 V_2}{(r_1 + r_2 + d)^6}, \quad (8)$$

exhibiting the material enhancement factor but a suboptimal distance dependence. The radiative transfer between two quasistatic spheres is known analytically [4]; on resonance, it is given approximately by Eq. (8), thereby reaching the limit.

Heat transfer between a dipole and a plate approaches the limit of Eq. (5), falling short by a factor of two due to polarization mismatch (surface resonances are supported for TM polarization only [61]). Integrating over the half-space occupied by any extended structure yields a maximum flux rate,

$$[\Phi(\omega)]_{\text{dipole-to-ext}} \leq \frac{1}{8\pi^2} \frac{|\chi_1(\omega)|^2 |\chi_2(\omega)|^2}{\text{Im } \chi_1(\omega) \text{Im } \chi_2(\omega)} \frac{V}{(r + d)^3} \quad (9)$$

where $r + d$ is the distance between the extended structure and the center of mass of the particle. The heat exchange between a quasistatic sphere and a bulk metal [4][SM] can achieve half of this maximum flux as long as the geometric or material resonant frequencies align.

Fig. 2 depicts flux rates for the sphere–sphere and sphere–plate geometries, computed by the fluctuating-surface current method [44, 46, 62], along with the limits of Eqs. (8,9). The spheres are modeled by Drude susceptibilities with plasma frequency ω_p and loss rate $\gamma = 0.1\omega_p$. The “plate” is modeled by a very large ellipsoid (volume $\approx 7000 \times$ larger than the sphere) comprising a material with a modified plasma frequency, $\omega_{p,\text{pl}} = \sqrt{2/3}\omega_p$ and a modified loss rate, $\gamma_{\text{pl}} = 2\gamma/3$, to align the resonance frequencies of the sphere and plate without modifying the extended-structure limit. In each case the separation distance $d = 0.1c/\omega_{\text{res}}$ and the spheres have radii $r = d/5$. The computations support the quasistatic analytical results discussed above and show that the dipolar limits can be approached to within at least a factor of two.

Extended Structures.—In contrast to dipolar interactions, we find that the heat transfer between common planar structures falls significantly short of the extended-structure limits. This occurs due to destructive-interference effects between the structures, and because translationally invariant structures necessarily exhibit resonances at $|\chi_{\text{eff}}| \approx 2$, preventing gains

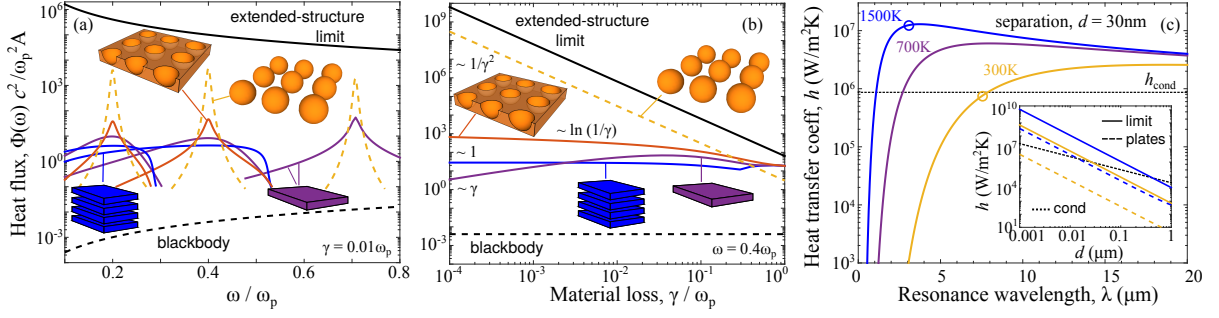


FIG. 3. (a,b) Comparison of heat flux for large-area Drude-metal structures. (a) Structures optimized for maximum flux at three frequencies, $\omega = (0.2, 0.4, 1/\sqrt{2})\omega_p$, for a loss rate $\gamma = 0.01\omega_p$. Thin films (purple), hyperbolic metamaterials (gold), and elliptical metamaterials (red) exceed black-body enhancements but fall far short of the limit (black) from Eq. (6). Bulk media (purple) have resonances at $\omega = \omega_p/\sqrt{2}$. The dashed gold line represents the heat transfer for a hypothetical plasmonic-particle array in the Born approximation. (b) Optimized structures as a function of loss rate, for $\omega = 0.4\omega_p$. Each structure exhibits the $1/d^2$ near-field enhancement factor, but none exhibit the $|\chi|^4/(\text{Im } \chi)^2 \sim 1/\gamma^2$ material enhancement factor except the idealized plasmonic-particle array. (c) Radiative heat transfer coefficient of a structure that reaches the limit in Eq. (6), for a bandwidth $\Delta\omega \propto \gamma$. Radiative heat exchange in this limit shows the possibility of surpassing conductive heat transfer through air (dotted) at 300K (gold), which is not possible for plate-plate configurations (inset, dashed), and of significant further enhancements at higher temperatures (blue, purple).

from large $|\chi|^4$. Structured surfaces with strong local interactions may be able to overcome these limitations.

The near-field heat transfer between two semi-infinite metals is maximum at the surface-plasmon frequency of the metals, but it is not linear in $|\chi|^4/(\text{Im } \chi)^2$, as it is for dipole-plate transfer in Eq. (9). Instead, as the plates approach each other, the resonances transition to metal-insulator-metal modes, with energy levels split around the single-surface plasmon energies [61]. The result is a weakened interaction and a maximum spectral heat flux at ω_{sp} of [SM]

$$\left[\frac{\Phi(\omega_{\text{sp}})}{A} \right]_{\text{plate-to-plate}} = \frac{1}{4\pi^2 d^2} \ln \left[\frac{|\chi|^4}{4(\text{Im } \chi)^2} \right] \quad (10)$$

which is similar to the limit in Eq. (6) except for the weak logarithmic material enhancement, $\Phi \sim \ln [|\chi|^4/(\text{Im } \chi)^2]$. Eq. (10) is compared to previous planar limits [10, 37] in the Supp. Mat. [SM].

It is possible to create low-frequency resonances, away from the surface-plasmon frequency of a metal, by reducing the volume fraction of metal, via either metamaterial or thin-film geometries. However, neither offers the possibility of approaching our limits. The maximum flux rate between hyperbolic metamaterials [25] (HMMs) is proportional to $1/d^2$ but independent of the underlying material [SM]. Optimal thin films behave similarly to HMMs [21], thereby also falling short of the limits. ‘‘Elliptical’’ metamaterials, with nearly isotropic negative effective susceptibilities (and therefore ellipsoidal isofrequency contours), exhibit resonances at $\chi_{\text{eff}} \approx -2$ and thus transfer heat at a rate limited by Eq. (10). They fall short of the limit due to the same interference effects present in bulk media, and because $|\chi_{\text{eff}}|^4 \ll |\chi|^4$.

Fig. 3(a,b) shows the heat flux between mirror images of optimized thin-film (purple), hyperbolic-metamaterial (gold), and elliptical-metamaterial (red) structures, as a function of

(a) frequency and (b) material-loss rate. For a Drude metal (plasma frequency ω_p) with $\gamma = 0.01\omega_p$, the thin-film thickness and metamaterial fill-fraction are optimized for maximum flux at multiple frequencies using a free-software implementation [64] of a local, derivative-free optimization algorithm [65]. In Fig. 3(b) the frequency is fixed at $\omega = 0.4\omega_p$ and the structures are optimized as a function of the loss rate γ . The maximum plate-plate flux rate is well-approximated by Eq. (10), and none of the conventional structures exhibits the material enhancement factor.

Additionally included in Fig. 3(a,b) is an idealized structure intended to be suggestive of how to approach the limits presented here. The structure comprises periodic ellipsoids (orange), operating *not* in the effective-medium limit but in an ‘‘additive’’ Born-approximation limit. The heat transfer is a lattice sum of dipole-dipole interactions given by Eq. (8), modified to account for incomplete coupling of polarizations along the minor semiaxes. The individual plasmonic nanoparticle resonances exhibit the metal enhancement factor $|\chi|^4/(\text{Im } \chi)^2$, as seen in Fig. 3(b), while the interactions across the lattice contribute to a $1/d^2$ near-field enhancement. Assuming close-packed particles with optimal size dimensions (restricted to be smaller than d), Fig. 3(a) suggests the possibility for two to three orders of magnitude enhancement by periodic structuring and tailored local interactions.

Finally, Fig. 3(c) shows the heat-transfer coefficient $h = \int \Phi(\partial\Theta/\partial T)d\omega$, or the heat conductance per area [4], for an extended structure that reaches the limits. We use a Drude material with frequency ω_p and loss rate $\gamma = 0.01\omega_p$ (appropriate e.g. for silver and gold [66]), and assume that the single-frequency limit given by Eq. (6) is reached at a tunable resonant frequency $\omega_{\text{res}} = \omega_p/\sqrt{2}$, with a bandwidth $\Delta\omega = \gamma/2$ (given by the inherent material loss [67, 68] and in agreement with dipole-dipole heat exchange [SM]). We find that at a separation distance $d = 50\text{nm}$, radiative heat trans-

fer can surpass conductive transfer across an air gap (assuming thermal conductivity $\kappa_{\text{air}} = 0.026\text{W/m}\cdot\text{K}$ [69]), even at 300K temperature. Higher temperatures would enable further (orders of magnitude) improvements. At 1500K, for example, radiative transfer could be the dominant mechanism even out to almost $d = 0.5\mu\text{m}$ (inset), whereas known plate–plate structures would require sub-10nm separations.

We thank Athanasios Polimeridis for helpful discussions. This work was supported by the Army Research Office through the Institute for Soldier Nanotechnologies under Contract No. W911NF-07-D0004, and by the AFOSR Multidisciplinary Research Program of the University Research Initiative (MURI) for Complex and Robust On-chip Nanophotonics under Grant No. FA9550-09-1-0704.

-
- [1] D. Polder and M. Van Hove, “Theory of Radiative Heat Transfer between Closely Spaced Bodies,” *Physical Review B* **4**, 3303–3314 (1971).
- [2] Sergej M. Rytov, Yurii A. Kravtsov, and Valeryan I. Tatarskii, *Principles of statistical radiophysics* (Springer-Verlag New York Inc., New York, NY, 1988).
- [3] Jean-Philippe Mulet, Karl Joulain, Rémi Carminati, and Jean-Jacques Greffet, “Enhanced Radiative Heat Transfer at Nanometric Distances,” *Microscale Thermophysical Engineering* **6**, 209–222 (2002).
- [4] Karl Joulain, Jean-Philippe Mulet, François Marquier, Rémi Carminati, and Jean-Jacques Greffet, “Surface electromagnetic waves thermally excited: Radiative heat transfer, coherence properties and Casimir forces revisited in the near field,” *Surface Science Reports* **57**, 59–112 (2005).
- [5] A. I. Volokitin and B. N. J. Persson, “Near-field radiative heat transfer and noncontact friction,” *Reviews of Modern Physics* **79**, 1291–1329 (2007).
- [6] Emmanuel Rousseau, Alessandro Siria, Guillaume Jourdan, Sebastian Volz, Fabio Comin, Joël Chevrier, and Jean-Jacques Greffet, “Radiative heat transfer at the nanoscale,” *Nature Photonics* **3**, 514–517 (2009).
- [7] S. Basu, Z. M. Zhang, and C. J. Fu, “Review of near-field thermal radiation and its application to energy conversion,” *International Journal of Energy Research* **33**, 1203–1232 (2009).
- [8] Jackson J. Loomis and Humphrey J. Maris, “Theory of heat transfer by evanescent electromagnetic waves,” *Physical Review B* **50**, 18517–18524 (1994).
- [9] J. B. Xu, K. Lauger, R. Moller, K. Dransfeld, and I. H. Wilson, “Heat transfer between two metallic surfaces at small distances,” *Journal of Applied Physics* **76**, 7209–7216 (1994).
- [10] J. B. Pendry, “Radiative exchange of heat between nanostructures,” *Journal of Physics: Condensed Matter* **11**, 6621–6633 (1999).
- [11] C.J. Fu and Z.M. Zhang, “Nanoscale radiation heat transfer for silicon at different doping levels,” *International Journal of Heat and Mass Transfer* **49**, 1703–1718 (2006).
- [12] Lu Hu, Arvind Narayanaswamy, Xiaoyuan Chen, and Gang Chen, “Near-field thermal radiation between two closely spaced glass plates exceeding Planck’s blackbody radiation law,” *Applied Physics Letters* **92**, 133106 (2008).
- [13] R. S. Ottens, V. Quetschke, Stacy Wise, A. A. Alemi, R. Lundock, G. Mueller, D. H. Reitze, D. B. Tanner, and B. F. Whiting, “Near-field radiative heat transfer between macroscopic planar surfaces,” *Physical Review Letters* **107**, 014301 (2011), arXiv:1103.2389.
- [14] P. J. Van Zwol, K. Joulain, P. Ben-Abdallah, and J. Chevrier, “Phonon polaritons enhance near-field thermal transfer across the phase transition of VO₂,” *Physical Review B* **84**, 1–4 (2011).
- [15] S.-A. Biehs, D. Reddig, and M. Holthaus, “Thermal radiation and near-field energy density of thin metallic films,” *The European Physical Journal B* **55**, 237–251 (2007).
- [16] Mathieu Francoeur, M. Pinar Menguc, and Rodolphe Vaillon, “Near-field radiative heat transfer enhancement via surface phonon polaritons coupling in thin films,” *Applied Physics Letters* **93**, 043109 (2008).
- [17] Mathieu Francoeur, M. Pinar Mengüç, and Rodolphe Vaillon, “Solution of near-field thermal radiation in one-dimensional layered media using dyadic Green’s functions and the scattering matrix method,” *Journal of Quantitative Spectroscopy and Radiative Transfer* **110**, 2002–2018 (2009).
- [18] Philippe Ben-Abdallah, Karl Joulain, Jmie Drevillon, and Gilberto Domingues, “Near-field heat transfer mediated by surface wave hybridization between two films,” *Journal of Applied Physics* **106**, 044306 (2009).
- [19] Mathieu Francoeur, M Pinar Mengüç, and Rodolphe Vaillon, “Spectral tuning of near-field radiative heat flux between two thin silicon carbide films,” *Journal of Physics D: Applied Physics* **43**, 075501 (2010).
- [20] Soumyadipta Basu and Mathieu Francoeur, “Maximum near-field radiative heat transfer between thin films,” *Applied Physics Letters* **98**, 243120 (2011).
- [21] Owen D. Miller, Steven G. Johnson, and Alejandro W. Rodriguez, “Effectiveness of Thin Films in Lieu of Hyperbolic Metamaterials in the Near Field,” *Physical Review Letters* **112**, 157402 (2014).
- [22] S.-A. Biehs, P. Ben-Abdallah, F. S. S. Rosa, K. Joulain, and J.-J. Greffet, “Nanoscale heat flux between nanoporous materials,” *Optics Express* **19**, A1088 (2011).
- [23] Mathieu Francoeur, Soumyadipta Basu, and Spencer J. Petersen, “Electric and magnetic surface polariton mediated near-field radiative heat transfer between metamaterials made of silicon carbide particles,” *Optics Express* **19**, 18774 (2011).
- [24] Karl Joulain, Jeremie Drevillon, and Philippe Ben-Abdallah, “Noncontact heat transfer between two metamaterials,” *Physical Review B* **81**, 165119 (2010).
- [25] S.-A. Biehs, M. Tschikin, and P. Ben-Abdallah, “Hyperbolic Metamaterials as an Analog of a Blackbody in the Near Field,” *Physical Review Letters* **109**, 104301 (2012).
- [26] S.-A. Biehs, M. Tschikin, R. Messina, and P. Ben-Abdallah, “Super-Planckian near-field thermal emission with phonon-polaritonic hyperbolic metamaterials,” *Applied Physics Letters* **102**, 131106 (2013).
- [27] Yu Guo and Zubin Jacob, “Thermal hyperbolic metamaterials,” *Optics Express* **21**, 15014–15019 (2013).
- [28] Evgenii E. Narimanov and Igor I. Smolyaninov, “Beyond Stefan-Boltzmann Law : Thermal Hyper-Conductivity,” in *Quantum Electronics and Laser Science Conference* (Optical Society of America, 2012).
- [29] MacMurray D. Whale and Ernest G. Cravalho, “Modeling and performance of microscale thermophotovoltaic energy conversion devices,” *IEEE Transactions on Energy Conversion* **17**, 130–142 (2002).
- [30] M. Laroche, R. Carminati, and J.-J. Greffet, “Near-field thermophotovoltaic energy conversion,” *Journal of Applied Physics* **100**, 063704 (2006).

- [31] Peter Bermel, Michael Ghebregbrhan, Walker Chan, Yi Xiang Yeng, Mohammad Araghchini, Raffif Hamam, Christopher H. Marton, Klavs F. Jensen, Marin Soljačić, John D. Joannopoulos, Steven G. Johnson, and Ivan Celanovic, "Design and global optimization of high-efficiency thermophotovoltaic systems." *Optics Express* **18**, A314–A334 (2010).
- [32] Alejandro W. Rodriguez, Ognjen Ilic, Peter Bermel, Ivan Celanovic, John D. Joannopoulos, Marin Soljačić, and Steven G. Johnson, "Frequency-Selective Near-Field Radiative Heat Transfer between Photonic Crystal Slabs: A Computational Approach for Arbitrary Geometries and Materials," *Physical Review Letters* **107**, 114302 (2011).
- [33] John H. Lienhard IV and John H. Lienhard V, *A Heat Transfer Textbook*, 4th ed. (Dover, 2011).
- [34] Craig F. Bohren and Donald R. Huffman, *Absorption and Scattering of Light by Small Particles* (John Wiley & Sons, New York, NY, 1983).
- [35] Steven G. Johnson, Peter Bienstman, M. A. Skorobogatiy, Mihai Ibanescu, Eleftherios Lidorikis, and J. D. Joannopoulos, "Adiabatic theorem and continuous coupled-mode theory for efficient taper transitions in photonic crystals," *Physical Review E* **66**, 066608 (2002).
- [36] S. Basu and Z. M. Zhang, "Maximum energy transfer in near-field thermal radiation at nanometer distances," *Journal of Applied Physics* **105**, 093535 (2009).
- [37] Philippe Ben-Abdallah and Karl Joulain, "Fundamental limits for noncontact transfers between two bodies," *Physical Review B* **82**, 121419 (2010), [arXiv:1009.4598](https://arxiv.org/abs/1009.4598).
- [38] Elyes Nefzaoui, Younès Ezzahri, Jérémie Drévilion, and Karl Joulain, "Maximal near-field radiative heat transfer between two plates," *The European Physical Journal Applied Physics* **63**, 30902 (2013), [arXiv:1302.1718](https://arxiv.org/abs/1302.1718).
- [39] Arvind Narayanaswamy and Gang Chen, "Thermal near-field radiative transfer between two spheres," *Physical Review B* **77**, 075125 (2008), [arXiv:0909.0765](https://arxiv.org/abs/0909.0765).
- [40] Jean Philippe Mulet, Karl Joulain, Rémi Carminati, and Jean Jacques Greffet, "Nanoscale radiative heat transfer between a small particle and a plane surface," *Applied Physics Letters* **78**, 2931–2933 (2001).
- [41] Arvind Narayanaswamy, Sheng Shen, and Gang Chen, "Near-field radiative heat transfer between a sphere and a substrate," *Physical Review B* **78**, 115303 (2008), [arXiv:0909.0784](https://arxiv.org/abs/0909.0784).
- [42] Sheng Shen, Arvind Narayanaswamy, and Gang Chen, "Surface Phonon Polaritons Mediated Energy Transfer Between Nanoscale Gaps," *Nano Letters* **9**, 2909–13 (2009).
- [43] Clayton Otey and Shanhui Fan, "Numerically exact calculation of electromagnetic heat transfer between a dielectric sphere and plate," *Physical Review B* **84**, 245431 (2011), [arXiv:1103.2668](https://arxiv.org/abs/1103.2668).
- [44] Alejandro W. Rodriguez, M. T. Homer Reid, and Steven G. Johnson, "Fluctuating-surface-current formulation of radiative heat transfer for arbitrary geometries," *Physical Review B* **86** (2012), [10.1103/PhysRevB.86.220302](https://arxiv.org/abs/10.1103/PhysRevB.86.220302), [arXiv:1206.1772v2](https://arxiv.org/abs/1206.1772v2).
- [45] Alexander P. McCauley, M. T. Homer Reid, Matthias Krüger, and Steven G. Johnson, "Modeling near-field radiative heat transfer from sharp objects using a general three-dimensional numerical scattering technique," *Physical Review B* **85** (2012), [10.1103/PhysRevB.85.165104](https://arxiv.org/abs/10.1103/PhysRevB.85.165104).
- [46] Alejandro W. Rodriguez, M. T. Homer Reid, and Steven G. Johnson, "Fluctuating-surface-current formulation of radiative heat transfer: Theory and applications," *Physical Review B* **88**, 054305 (2013).
- [47] Clayton R. Otey, Linxiao Zhu, Sunil Sandhu, and Shanhui Fan, "Fluctuational electrodynamics calculations of near-field heat transfer in non-planar geometries: A brief overview," *Journal of Quantitative Spectroscopy and Radiative Transfer* **132**, 3–11 (2014).
- [48] Jin Au Kong, *Theory of electromagnetic waves*, Vol. 1 (Wiley-Interscience, New York, NY, 1975).
- [49] D. A. B. Miller, "Communicating with waves between volumes: evaluating orthogonal spatial channels and limits on coupling strengths." *Applied Optics* **39**, 1681–1699 (2000).
- [50] V Adrian Parsegian, *Van der Waals forces: a handbook for biologists, chemists, engineers, and physicists* (Cambridge University Press, 2005).
- [51] Aaron Welters, Yehuda Avniel, and Steven G. Johnson, "Speed-of-light limitations in passive linear media," *Physical Review A* **90**, 023847 (2014).
- [52] Owen D. Miller, Athanasios G. Polimeridis, M. T. Homer Reid, Chia Wei Hsu, Brendan G. DeLacy, John D. Joannopoulos, Marin Soljačić, and Steven G. Johnson, "Fundamental limits to the optical response of lossy media," Submitted (2015), [arXiv:1503.03781](https://arxiv.org/abs/1503.03781).
- [53] E. J. Rothwell and M. J. Cloud, *Electromagnetics* (CRC Press LLC, 2001).
- [54] J. D. Jackson, *Classical Electrodynamics, 3rd Ed.* (John Wiley & Sons, Inc., 1999).
- [55] Roger G. Newton, "Optical theorem and beyond," *American Journal of Physics* **44**, 639 (1976).
- [56] D. Lytle, P. Carney, John Schotland, and Emil Wolf, "Generalized optical theorem for reflection, transmission, and extinction of power for electromagnetic fields," *Physical Review E* **71**, 056610 (2005).
- [57] Hila Hashemi, Cheng-Wei Qiu, Alexander P. McCauley, J. D. Joannopoulos, and Steven G. Johnson, "Diameter-bandwidth product limitation of isolated-object cloaking," *Physical Review A* **86**, 013804 (2012).
- [58] Weng Cho Chew, *Waves and fields in inhomogeneous media*, Vol. 522 (IEEE press New York, 1995).
- [59] Lloyd N. Trefethen and David Bau, *Numerical Linear Algebra* (Society for Industrial and Applied Mathematics, Philadelphia, PA, 1997).
- [60] Rafael Piestun and David A. B. Miller, "Electromagnetic degrees of freedom of an optical system," *Journal of the Optical Society of America A* **17**, 892 (2000).
- [61] Stefan Alexander Maier, *Plasmonics: fundamentals and applications* (Springer Science & Business Media, 2007).
- [62] M. T. Homer Reid, "scuff-EM: Free, open-source boundary-element software," <http://homerreid.com/scuff-EM>.
- [63] J. C. Maxwell Garnett, "Colours in metal glasses, in metallic films, and in metallic solutions. II," *Philosophical Transactions of the Royal Society of London Series A* **205**, 237–288 (1906).
- [64] Steven G. Johnson, "The NLOpt nonlinear-optimization package," <http://ab-initio.mit.edu/nlopt>.
- [65] Michael J. D. Powell, "A direct search optimization method that models the objective and constraint functions by linear interpolation," in *Advances in Optimization and Numerical Analysis* (Springer, 1994) pp. 51–67.
- [66] Edward D. Palik, *Handbook of Optical Constants of Solids*, edited by E. D. Palik (Elsevier Science, 1998).
- [67] Feng Wang and Y. Ron Shen, "General Properties of Local Plasmons in Metal Nanostructures," *Physical Review Letters* **97**, 206806 (2006).
- [68] Aaswath Raman, Wonseok Shin, and Shanhui Fan, "Upper Bound on the Modal Material Loss Rate in Plasmonic and Metamaterial Systems," *Physical Review Letters* **110**, 183901 (2013).
- [69] William M Haynes, *CRC handbook of chemistry and physics* (CRC press, 2013).

Supplementary Materials: Shape-independent limits to near-field radiative heat transfer

Owen D. Miller,¹ Steven G. Johnson,¹ and Alejandro W. Rodriguez²

¹*Department of Mathematics, Massachusetts Institute of Technology, Cambridge, MA 02139*

²*Department of Electrical Engineering, Princeton University, Princeton, NJ 08544*

We provide: (1) a derivation and discussion of the higher-order terms in the heat flux limits, which tend to be very small for near-field heat transfer, (2) a derivation of the maximum attainable heat flux between two thin films, for a given material, (3) a derivation of the limits for a very general class of materials, and (4) a derivation of the radiative heat transfer coefficient if the limiting flux rates are achieved, alongside a comparison to conductive heat transfer through air.

I. EVALUATION OF INTEGRAL LIMITS AND HIGHER-ORDER TERMS

In this section, we present calculations and clarify the step needed to go from Eq. (5) to Eq. (6) of the main text. Specifically, Eq. (5) is an integral bound that applies to any near- or far-field interactions, depending only on conservation of energy arguments. Eq. (6) simplifies the bound for the case of near-field heat transfer by assuming that the near-field quasistatic $1/r^3$ term in \mathbf{G}_0 is the dominant term and integrating over the infinite half-spaces occupied by the two bodies. (All equations and figures in this Supplementary Material are preceded with an “S,” whereas equations and figures without an “S” refer to the main text.) Here we justify dropping the $1/r^2$ and $1/r$ terms in the Green’s function. Although for many structures it is known that optimal near-field heat transfer is governed by high-wavevector waves corresponding to the $1/r^3$ term, the mathematical justification for dropping the terms is somewhat subtle. Integrated over infinite half-spaces, the two terms diverge. We show that this divergence is unphysical—originating from the optimal variational fields that are appropriate in the near field but which do not satisfy Maxwell’s equations in the far field. Moreover, we show that for finite, reasonable interaction distances, their contributions are negligible compared to the contribution of the $1/r^3$ term. As shown in the text, the limit of Eq. (5), keeping only the $1/r^3$ term, yields very good agreement with the response of sphere–sphere and sphere–plate interactions.

The squared Frobenius norm of the homogeneous Green’s function is:

$$\|\mathbf{G}_0\|_F^2 = \frac{k^6}{8\pi^2} \left[\frac{3}{(kr)^6} + \frac{1}{(kr)^4} + \frac{1}{(kr)^2} \right] \quad (\text{S.1})$$

which has contributions from $1/r^6$, $1/r^4$, and $1/r^2$ terms. For convenience, instead of taking infinite half-spaces, we assume that both bodies are contained within a circular cylinder of radius R and height L . The integral of the norm over both volumes is a six-dimensional integral, but we bound it above by fixing the source in one body at its center ($x = y = 0$), and multiplying by the cylindrical area $A = \pi R^2$:

$$\int_{V_1, V_2} \|\mathbf{G}_0\|_F^2 \leq A \int dz_1 \int dz_2 \int d\rho_2 \pi \rho \|\mathbf{G}_0\|_F^2 \quad (\text{S.2})$$

where we have further simplified the integral using cylindrical coordinates. The multiplication by A is exact for (in-

finitely wide) structures with translational and rotational symmetry; since we are interested in global bounds encompassing large structures it is thus a good approximation. The bound in Eq. (6) of the main text comes from the $1/r^6$ term in the GF for an infinite volume (it is very weakly decreased for large but finite structures). The integral is given by:

$$\int_{V'_1, V'_2} \frac{3}{r^6} = \frac{\pi A}{8d^2}, \quad (\text{S.3})$$

where V'_1 and V'_2 are the infinite half-spaces containing the bodies. Multiplying by the prefactors in Eq. (S.1) yields the bound in Eq. (6) of the main text. Over finite volumes, the second term is more complicated:

$$\begin{aligned} \int_{V_1, V_2} \frac{1}{r^4} = & \pi A \left[\log \left[\frac{(d+L)^2}{d(d+2L)} \right] - \frac{2L+d}{R} \tan^{-1} \left(\frac{2L+d}{R} \right) \right. \\ & \left. + 2 \frac{L+d}{R} \tan^{-1} \left(\frac{L+d}{R} \right) \right. \\ & \left. + \frac{1}{2} \log \left[\frac{((2L+d)^2 + R^2)(d^2 + R^2)}{((L+d)^2 + R^2)^2} \right] - \frac{d}{R} \tan^{-1} \left(\frac{d}{R} \right) \right] \quad (\text{S.4}) \end{aligned}$$

The third term is given by:

$$\begin{aligned} \int_{V_1, V_2} \frac{1}{r^2} = & \pi A \left[\frac{R^2}{2} \log \left[\frac{((L+d)^2 + R^2)^2}{((2L+d)^2 + R^2)(R^2 + d^2)} \right] \right. \\ & \left. + \frac{(2L+d)^2}{2} \log \left[1 + \frac{R^2}{(2L+d)^2} \right] \right. \\ & \left. - (L+d)^2 \log \left[1 + \frac{R^2}{(L+d)^2} \right] + \frac{d^2}{2} \log (1 + R^2/d^2) \right. \\ & \left. + 2R(d+2L) \tan^{-1} \left(\frac{d+2L}{R} \right) \right. \\ & \left. - 4R(d+L) \tan^{-1} \left(\frac{d+L}{R} \right) + 2Rd \tan^{-1} \left(\frac{d}{R} \right) \right] \quad (\text{S.5}) \end{aligned}$$

Eqs. (S.4,S.5) are difficult to disentangle so we consider large but finite volumes. Large bodies satisfy

$$L, R \gg d \quad (\text{S.6})$$

such that their sizes are much larger than their spacing. Not only do L and R represent the physical sizes of the bodies,

they also represent the interaction sizes: they are the volumes over which polarization currents within the respective bodies transfer energy. Near-field interactions by definition occur between charges or currents at the subwavelength scale, such that one is typically interested in sizes $L \ll \lambda$. Conversely, surface waves between structures are example of coherent subwavelength interactions that potentially take place over distances much greater than the wavelength, $R \gg \lambda$. Thus the finite-but-large asymptotic expansion relevant for near-field heat transfer can be made by taking

$$d \ll L \ll R \quad (\text{S.7})$$

for the two circular cylinders with radii R , heights L , and separation distance d . In this asymptotic limit, the terms simplify:

$$\frac{1}{\pi A} \int_{V'_1, V'_2} \frac{3}{r^6} = \frac{1}{8d^2} \quad (\text{S.8})$$

$$\frac{1}{\pi A} \int_{V_1, V_2} \frac{1}{r^4} \approx \log\left(\frac{L}{2d}\right) \quad (\text{S.9})$$

$$\frac{1}{\pi A} \int_{V_1, V_2} \frac{1}{r^2} \approx 2L^2 \log\left(\frac{R}{4L}\right) \quad (\text{S.10})$$

The divergences in the second and third terms are relatively weak. The second term is negligible compared to the third term, which tends to be very small compared to the first. The comparison between the first and third term essentially compares $1/(kd)^2$ versus $(kL)^2$; even in a generous upper bound in which $kL \approx 1$, the third term is still much smaller than $1/(kd)^2 \gg 1$. In Table 1 we compare the bound arising from Eq. (6) to the bound that would arise from adding Eqs. (S.4,S.5) to Eq. (6). We see that for near-field distances ($d \ll \lambda$), even very large estimates of the interaction distances L and R lead to only small modifications to the upper limit, on the order of 1% and in some cases significantly smaller.

kd	kL	kR	Eq. (6)	Eq. (6)+Eqs. (S.4,S.5)	Rel. Error
0.01	1	1	1250	1252	0.17%
0.01	1	10	1250	1254	0.35%
0.01	1	100	1250	1256	0.53%
0.001	1	100	1.25×10^5	1.25008×10^5	0.0063%
0.001	10	1000	1.25×10^5	1.255×10^5	0.38%

Finally, we note that these divergences arise even for far-field interactions, where they are clearly unphysical because finite blackbody limits to the flux per unit area are well known. The unphysical divergences arise from the assumption that the optimal polarization fields are proportional to the incident fields. Such a condition is ideal and achievable for the $1/r^3$ contribution of \mathbf{G}_0 that typically dominates near-field transfer, but is unphysical for the more slowly decaying $1/r^2$ and $1/r$ terms: a constant energy flux is maintained in a lossy medium over large length scales, which is physically impossible. One approach would be to “split” the problem into near- and far-field contributions, and to bound the interactions separately. However, given the relatively weak nature of these

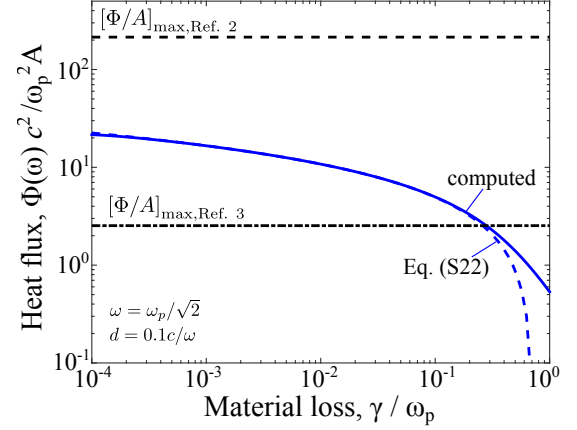


FIG. S1. Heat flux per unit area of two Drude-metal bulk media as a function of material loss rate, γ/ω_p , at the resonant frequency $\omega = \omega_p/\sqrt{2}$ and at a fixed separation of $d = 0.1c/\omega$. Except for very large loss, the heat flux approaches the approximate rate of Eq. (S.22), confirming the logarithmic dependence on the material loss rate. Conversely, the limit of Ref. 2 is overly optimistic, and the “limit” of Ref. 3 is overly pessimistic. For the interatomic spacing that enters the limit of Ref. 2, we took $b/\lambda \approx 1/1000$, which is appropriate e.g. for silver.

contributions for finite interaction distances ($< 1\%$), they can be ignored for near-field radiative heat transfer, justifying the use of Eq. (6) in the main text.

II. HEAT TRANSFER BETWEEN BULK PLANAR MEDIA

We derive the optimal heat-transfer rate between two planar bodies comprising a material of susceptibility $\chi(\omega)$, corresponding to Eq. (10) of the main text. Ref. 1 assumed a frequency-independent susceptibility, which they optimized for maximum heat transfer, whereas we assume a fixed (possibly frequency-dependent) susceptibility. Ref. 2 and Ref. 3 also provide expressions for optimal heat flux between planar bodies, but their limits require wavevector-dependent material properties. The limits in both Ref. 2 and Ref. 3 arise only because a finite maximum surface-parallel wavevector magnitude (k_{\parallel}) is postulated: in Ref. 2 the maximum $k_{\parallel, \max} = 1/b$ is chosen, where b is the interatomic spacing of the metal; in Ref. 3, the maximum k_{\parallel} is inversely proportional to the gap spacing d , which does not account for large wavevectors that are possible when material losses are small. Although the interatomic spacing certainly sets an upper bound to the process as described by bulk materials, for lossy materials the loss is the limiting factor, not the interatomic spacing. We find a logarithmic dependence (and divergence) of the heat flux with the material loss rate, which we validate in Fig. S1.

The radiative heat flux $\Phi(\omega)$ between two planar slabs is given by [4]

$$\Phi(\omega) = \frac{A}{4\pi^2} \int_0^\infty dk_{\parallel} k_{\parallel} (T_p + T_s) \quad (\text{S.11})$$

where A is the area of the plates, k_{\parallel} is the magnitude of the surface-parallel part of the wavevector, and T_s and T_p represent the field transmissions from slab 1 to slab 2 for s and p polarizations, respectively. By symmetry, the surface-parallel wavevector k_{\parallel} is a conserved quantity between plane waves in each medium. The heat flux is characterized by a strong peak at a single k_{\parallel} (for a given ω) corresponding to the metal-insulator-metal plasmonic mode. We show that at a given frequency, the bandwidth in k_{\parallel} is approximately constant, while the peak energy transmission scales logarithmically with the inverse of the material loss rate.

In the near field, we can focus only on the p -polarized transmission coefficient for evanescent waves with $k_{\parallel} > k_0$. Assuming two slabs of the same material, with reflectivity r for waves incident from air, the transmission coefficient is [4]:

$$T_p = \frac{4 [\text{Im}(r)]^2 e^{-2\gamma d}}{|1 - r^2 e^{-2\gamma d}|^2} \quad (\text{S.12})$$

where $\gamma = k_{\parallel} \sqrt{1 - k_0^2/k_{\parallel}^2} \approx k_{\parallel}$, assuming $k_{\parallel} \gg k_0$. Without the denominator, Eq. (S.12) would yield a $|\chi|^4/(\text{Im} \chi)^2$ enhancement from the plasmon waves at each surface, manifested in the poles of $\text{Im} r_p$ [5]. However, at the small distances necessary to transfer energy, the denominator—heuristically originating from the infinite sum of reflected waves—has an identical pole that *cancels* the one in the numerator. The resonances of T_p are instead metal-insulator-metal modes, with energy levels split around the single-surface plasmon energies [6], as discussed in the main text.

Ref. 2 and Ref. 3 find limits to the transfer by noting that at every k_{\parallel} the maximum value of T is 1 (note that for conventional metals such a transmission would require a wavevector-dependent permittivity). They define $k_{p,\text{max}}^2 = 1/b^2$ [2] and $k_{p,\text{max}}^2 = 4/d^2$ [3], respectively, yielding limits:

$$\left[\frac{\Phi(\omega)}{A} \right]_{\text{max,Ref. 2}} = \frac{1}{8\pi^2 b^2} \quad (\text{S.13})$$

$$\left[\frac{\Phi(\omega)}{A} \right]_{\text{max,Ref. 3}} = \frac{1}{2\pi^2 d^2} \quad (\text{S.14})$$

for interatomic spacing b and separation distance d .

Instead we seek a limit assuming a conventional (wavevector-independent) material susceptibility $\chi(\omega)$. Defining $x = 2k_{\parallel}d$, the flux is given by:

$$\begin{aligned} \Phi(\omega) &= \frac{A}{4\pi^2 d^2} \int_0^{\infty} \frac{[\text{Im}(r)]^2 x e^{-x}}{1 - 2\text{Re}(r^2)e^{-x} + |r|^4 e^{-2x}} dx \\ &= \frac{A}{4\pi^2 d^2} \int_0^{\infty} x f(x) dx \end{aligned} \quad (\text{S.15})$$

where the integral lower bound can be set to zero because we have assumed $k_0 d \ll 1$, and $f(x)$ is defined by

$$f(x) = \frac{[\text{Im}(r)]^2 e^{-x}}{1 - 2\text{Re}(r^2)e^{-x} + |r|^4 e^{-2x}}. \quad (\text{S.16})$$

At large k_{\parallel} , the reflectivity r is approximately constant and given by $r = (\varepsilon - 1)/(\varepsilon + 1)$. We will not insert its exact

form at the moment, but we will note that for the optimal susceptibility (see below) the real part of r is 0 and the imaginary part is potentially large. If we define the average [weighted by $f(x)$] value of x as x_0 , it follows that $\int x f(x) = x_0 \int f(x)$ and hence Φ can be approximately given by:

$$\Phi(\omega) \approx \frac{x_0 A}{4\pi^2 d^2} \int_0^{\infty} f(x) dx \quad (\text{S.17})$$

The integral of f can be worked out:

$$\begin{aligned} \int_0^{\infty} f(x) dx &= \frac{[\text{Im}(r)]^2}{\text{Im}(r^2)} \left[\frac{\pi}{2} - \tan^{-1} \left(\frac{1 - \text{Re}(r^2)}{\text{Im}(r^2)} \right) \right] \\ &= \frac{[\text{Im}(r)]^2}{\text{Im}(r^2)} \tan^{-1} \left(\frac{\text{Im}(r^2)}{1 - \text{Re}(r^2)} \right) \\ &\approx \frac{[\text{Im}(r)]^2}{1 - \text{Re}(r^2)} \end{aligned} \quad (\text{S.18})$$

where we used $\tan^{-1}(1/x) = \pi/2 - \tan^{-1}(x)$, and for x small, $\tan^{-1}(x) \approx x$. For the final step, we can write $\text{Re}(r^2) = [\text{Re}(r)]^2 - [\text{Im}(r)]^2 = 1 - [\text{Im}(r)]^2$. To find the value of x_0 , we approximate it (verifying later) as the value of x at which $f(x)$ peaks. Setting the derivative of f in Eq. (S.16) to zero yields:

$$x_0 = \ln |r|^2. \quad (\text{S.19})$$

Because $r = 1/[1 + 2/\chi(\omega)]$, the optimal frequency for maximum $|r|$ is given by the frequency such that $\text{Re}(-1/\chi(\omega)) = 1/2$. At this frequency, $r = i|\chi|^2/2\text{Im} \chi$ and we have:

$$x_0 = \ln \left[\frac{|\chi|^4}{4(\text{Im} \chi)^2} \right] \quad (\text{S.20})$$

$$\int_0^{\infty} f(x) dx = 1 \quad (\text{S.21})$$

Thus at the optimal frequency, maximum energy transmission occurs for k_{\parallel} logarithmically proportional to the inverse of the material loss rate, and the bandwidth in k_{\parallel} is constant. Hence, the radiative flux rate between the two slabs is given by:

$$\frac{\Phi(\omega)}{A} \approx \frac{1}{4\pi^2 d^2} \ln \left[\frac{|\chi|^4}{4(\text{Im} \chi)^2} \right] \quad (\text{S.22})$$

The asymptotic expression in Eq. (S.22) is almost identical to the limit in Eq. (10) in the main text, except that the flux rate scales logarithmically instead of linearly with $|\chi|^4/(\text{Im} \chi)^2$.

Conversely, for hyperbolic metamaterials, the optimal near-field heat flux is [7]

$$\left[\frac{\Phi(\omega_{\text{res}})}{A} \right]_{\text{HMM-to-HMM}} = \frac{\ln 2}{4\pi^2 d^2}. \quad (\text{S.23})$$

HMMs therefore do not exhibit any material enhancement; because the resonant modes are inside the bulk rather than at the surface, there is no divergence in the lossless limit.

III. LIMITS FOR GENERAL MEDIA

For clarity, and with regard to practical relevance, we presented in the main text only limits to heat flux for non-magnetic, isotropic bodies. Here we derive the limits for more general media, leading to the generalization $|\chi|^2/\text{Im}\chi \rightarrow \left\|(\text{Im}\boldsymbol{\xi})^{-1}\right\|_2$, for $\boldsymbol{\xi} = -\boldsymbol{\chi}^{-1}$, discussed in the main text.

The Maxwell curl equations are

$$\nabla \times \mathbf{H} + i\omega\mathbf{D} = \mathbf{J}_e \quad (\text{S.24})$$

$$-\nabla \times \mathbf{E} + i\omega\mathbf{B} = \mathbf{J}_m \quad (\text{S.25})$$

To simplify notation going forward, we will encapsulate electric and magnetic components of fields and currents into six-component vectors. We denote the fields by ψ , the free currents by σ , and the induced polarization currents by ν :

$$\psi = \begin{pmatrix} \mathbf{E} \\ \mathbf{H} \end{pmatrix} \quad \sigma = \begin{pmatrix} \mathbf{J}_e \\ \mathbf{J}_m \end{pmatrix} \quad \nu = \begin{pmatrix} \mathbf{P} \\ \mathbf{M} \end{pmatrix} \quad (\text{S.26})$$

The polarization currents within a body are related to the internal fields by the tensor susceptibility $\boldsymbol{\chi}$,

$$\nu = \boldsymbol{\chi}\psi. \quad (\text{S.27})$$

Given these definitions, the Maxwell curl equations can be rewritten:

$$\left[\begin{pmatrix} i\omega\varepsilon_0 & \nabla \times \\ -\nabla \times & i\omega\mu_0 \end{pmatrix} + i\omega\boldsymbol{\chi} \right] \psi = \sigma \quad (\text{S.28})$$

Following the derivation in the main text, the first step is to define a Green's function (GF), $\boldsymbol{\Gamma}_1$, in the presence of only body 1:

$$\left[\begin{pmatrix} i\omega\varepsilon_0 & \nabla \times \\ -\nabla \times & i\omega\mu_0 \end{pmatrix} + i\omega\boldsymbol{\chi}_1 \right] \boldsymbol{\Gamma}_1(\mathbf{x}, \mathbf{x}_0) = -i\omega\mathbf{I}\delta(\mathbf{x} - \mathbf{x}_0) \quad (\text{S.29})$$

where it is implicit that $\boldsymbol{\chi}_1 = 0$ at points outside of V_1 . Then the total fields in the presence of both bodies, excited by stochastic currents in body 1, satisfy the integral equation

$$\psi(\mathbf{x}) = \frac{i}{\omega} \int_{V_1} \boldsymbol{\Gamma}_1(\mathbf{x}, \mathbf{x}_0)\sigma(\mathbf{x}_0) + \int_{V_2} \boldsymbol{\Gamma}_1(\mathbf{x}, \mathbf{x}_0)\boldsymbol{\chi}_2\psi(\mathbf{x}_0) \quad (\text{S.30})$$

$$= \psi_{\text{inc},1} + \int_{V_2} \boldsymbol{\Gamma}_1(\mathbf{x}, \mathbf{x}_0)\boldsymbol{\chi}_2\psi(\mathbf{x}_0). \quad (\text{S.31})$$

Now the fields incident from body 1 have been separated from the ‘‘scattered’’ fields that arise only from the introduction of body 2, while fully accounting for interactions between the two bodies. Then the powers absorbed and extinguished by body 2 are given by:

$$P_{\text{abs}} = \frac{\omega}{2} \text{Im} \int_{V_2} \bar{\nu} \cdot \boldsymbol{\xi}_2 \nu \quad (\text{S.32})$$

$$P_{\text{ext}} = \frac{\omega}{2} \text{Im} \int_{V_2} \overline{\psi_{\text{inc},1}} \cdot \nu \quad (\text{S.33})$$

where

$$\boldsymbol{\xi}_2 = -\boldsymbol{\chi}_2^{-1} \quad (\text{S.34})$$

Constraining $P_{\text{abs}} < P_{\text{ext}}$ yields a limit to the absorbed power:

$$P_{\text{abs}} \leq \frac{\omega}{2} \int_{V_2} \overline{\psi_{\text{inc},1}} \cdot (\text{Im}\boldsymbol{\xi}_2)^{-1} \psi_{\text{inc},1} \quad (\text{S.35})$$

$$\leq \frac{\omega}{2} \left\| (\text{Im}\boldsymbol{\xi}_2)^{-1} \right\|_2 \int_{V_2} |\psi_{\text{inc},1}|^2 \quad (\text{S.36})$$

where the second inequality follows from the definition of the induced matrix 2-norm, $\|\cdot\|$. We can write out the squared magnitude of the incident field:

$$|\psi_{\text{inc},1}|^2 = \frac{1}{\omega^2} \int_{V_1} \int_{V_1} \sigma^\dagger(\mathbf{x}_1)\boldsymbol{\Gamma}_1^\dagger(\mathbf{x}, \mathbf{x}_1)\boldsymbol{\Gamma}_1(\mathbf{x}, \mathbf{x}'_1)\sigma(\mathbf{x}'_1) \quad (\text{S.37})$$

The fluctuation-dissipation theorem dictates that the ensemble average of the current-current correlation function is

$$\langle \sigma(\mathbf{x}'_1)\sigma^\dagger(\mathbf{x}_1) \rangle = \frac{4}{\pi} \omega [\text{Im}\boldsymbol{\chi}_1] \delta(\mathbf{x}_1 - \mathbf{x}'_1)\Theta(\omega, T_1) \quad (\text{S.38})$$

Inserting Eq. (S.38) into Eq. (S.37) yields the limit to the energy flux into body 2 (the Planck factor separately multiplies the flux to give the total power):

$$\Phi(\omega) \leq \frac{2}{\pi} \left\| (\text{Im}\boldsymbol{\xi}_2)^{-1} \right\|_2 \text{Tr} \int_{V_1} \int_{V_2} \boldsymbol{\Gamma}_1(\mathbf{x}_1, \mathbf{x}_2) (\text{Im}\boldsymbol{\chi}_1) \boldsymbol{\Gamma}_1^\dagger(\mathbf{x}_1, \mathbf{x}_2) \quad (\text{S.39})$$

The integrand in Eq. (S.39) relates the fields in V_2 , in empty space, from sources in V_1 , within body 1. To find limits to this quantity, it would be useful to transpose the source and measurement positions in the Green's functions. Even if body 1 consists of a nonreciprocal material, it is possible to switch the source and receiver positions if the material susceptibility,

$$\boldsymbol{\chi} = \begin{pmatrix} \chi_{11} & \chi_{12} \\ \chi_{21} & \chi_{22} \end{pmatrix} \quad (\text{S.40})$$

is simultaneously transformed to a *complementary* medium [8],

$$\boldsymbol{\chi}_C = \begin{pmatrix} \chi_{11}^T & -\chi_{21}^T \\ -\chi_{12}^T & \chi_{22}^T \end{pmatrix} \quad (\text{S.41})$$

$$= S\boldsymbol{\chi}^T S \quad (\text{S.42})$$

where

$$S = \begin{pmatrix} \mathbb{I} & \\ & -\mathbb{I} \end{pmatrix} \quad (\text{S.43})$$

and \mathbb{I} is the 3×3 identity matrix. Defining $\boldsymbol{\Gamma}_C$ as the Green's function in the presence of the complementary-medium body 1, the modified reciprocity relation [8] dictates:

$$\boldsymbol{\Gamma}_1(\mathbf{x}_1, \mathbf{x}_2) = S\boldsymbol{\Gamma}_C^T(\mathbf{x}_2, \mathbf{x}_1)S \quad (\text{S.44})$$

We can then perform a number of simplifications on the integrand in Eq. (S.39), including the trace operator and pulling the imaginary operator out front:

$$\begin{aligned}
& \text{Im Tr } \mathbf{\Gamma}_1(\mathbf{x}_1, \mathbf{x}_2) \boldsymbol{\chi}_1 \mathbf{\Gamma}_1^\dagger(\mathbf{x}_1, \mathbf{x}_2) \\
&= \text{Im Tr } S \mathbf{\Gamma}_C^T(\mathbf{x}_2, \mathbf{x}_1) S \boldsymbol{\chi}_1 S \bar{\mathbf{\Gamma}}_C(\mathbf{x}_2, \mathbf{x}_1) S \\
&= \text{Im Tr } S \mathbf{\Gamma}_C^T(\mathbf{x}_2, \mathbf{x}_1) \boldsymbol{\chi}_{1C}^T \bar{\mathbf{\Gamma}}_C(\mathbf{x}_2, \mathbf{x}_1) S \\
&= \text{Im Tr } \mathbf{\Gamma}_C^T(\mathbf{x}_2, \mathbf{x}_1) \boldsymbol{\chi}_{1C}^T \bar{\mathbf{\Gamma}}_C(\mathbf{x}_2, \mathbf{x}_1) \\
&= \text{Im Tr } \mathbf{\Gamma}_C^\dagger(\mathbf{x}_2, \mathbf{x}_1) \boldsymbol{\chi}_{1C} \mathbf{\Gamma}_C(\mathbf{x}_2, \mathbf{x}_1)
\end{aligned}$$

where the first equality uses reciprocity as defined by Eq. (S.44), the second equality uses the definition of the complementary medium, Eq. (S.42), the third equality uses $\text{Tr } S X S = \text{Tr } X$, by the definition of S , and the final equality takes the transpose of the matrix product inside the trace. After applying these transformations, Eq. (S.39) now represents a new absorption problem: the absorption inside the *complementary* version of body one due to sources in empty space in V_2 . This absorption problem can be bounded just as the previous one was, by energy conservation, such that

$$\text{Im} \int_{V_1} \mathbf{\Gamma}_C^\dagger(\mathbf{x}_2, \mathbf{x}_1) \boldsymbol{\chi}_{1C} \mathbf{\Gamma}_C(\mathbf{x}_2, \mathbf{x}_1) \quad (\text{S.45})$$

$$\leq \left\| (\text{Im } \boldsymbol{\xi}_{1C})^{-1} \right\|_2 \int_{V_1} \mathbf{\Gamma}_0^\dagger(\mathbf{x}_2, \mathbf{x}_1) \mathbf{\Gamma}_0(\mathbf{x}_2, \mathbf{x}_1) \quad (\text{S.46})$$

where $\mathbf{\Gamma}_0$ is the free-space Green's function and $\boldsymbol{\xi}_{1C} = -\boldsymbol{\chi}_{1C}^{-1}$. It turns out that the norm of the loss rate for the complementary material is equal to the norm of the loss rate of the original material:

$$\begin{aligned}
\left\| (\text{Im } \boldsymbol{\xi}_{1C})^{-1} \right\|_2 &= \left\| -(\text{Im } \boldsymbol{\chi}_{1C}^{-1})^{-1} \right\|_2 \\
&= \left\| -(\text{Im } [S \boldsymbol{\chi}_1^T S]^{-1})^{-1} \right\|_2 \\
&= \left\| -(\text{Im } [\boldsymbol{\chi}_1^T]^{-1})^{-1} \right\|_2 \\
&= \left\| -(\text{Im } [\boldsymbol{\chi}_1]^{-1})^{-1} \right\|_2 \\
&= \left\| (\text{Im } \boldsymbol{\xi}_1)^{-1} \right\|_2
\end{aligned}$$

through repeated application of the facts that $S^{-1} = S^\dagger = S$ and that transposing a matrix does not affect its norm. Finally, we relate the trace of the integrand to the Frobenius norm of the Green's function:

$$\text{Tr } \mathbf{\Gamma}_0^\dagger \mathbf{\Gamma}_0 = \|\mathbf{\Gamma}_0\|_F^2 \quad (\text{S.47})$$

to ultimately yield a flux limit:

$$\Phi(\omega) \leq \frac{2}{\pi} \left\| (\text{Im } \boldsymbol{\xi}_1)^{-1} \right\|_2 \left\| (\text{Im } \boldsymbol{\xi}_2)^{-1} \right\|_2 \int_{V_1} \int_{V_2} \|\mathbf{\Gamma}_0(\mathbf{x}_1, \mathbf{x}_2)\|_F^2 \quad (\text{S.48})$$

that is precisely the generalization of Eq. (5) in the main text, for a wide class of materials. The limit could even be extended to inhomogeneous media, although the exact geometry would need to be specified to know the material loss rate everywhere.

IV. RADIATIVE VS CONDUCTIVE HEAT-TRANSFER COEFFICIENTS

We compare radiative heat transfer to conductive heat transfer and derive the equations used for the plots shown in Fig. 3(c). The total radiative heat transfer between two bodies is given by Eq. (1) in the main text, $H = \int \Phi(\omega) [\Theta(\omega, T_1) - \Theta(\omega, T_2)] d\omega$. For a small temperature differential between the bodies, the conductance (heat transfer per unit temperature) per area A is termed the *radiative heat transfer coefficient* and is given by

$$h_{\text{rad}} = \frac{1}{A} \int \Phi(\omega) \frac{\partial \Theta}{\partial T} d\omega = \frac{1}{A} k_B \int \Phi(\omega) f(\omega) d\omega, \quad (\text{S.49})$$

where

$$f(\omega) = \left(\frac{\hbar\omega}{k_B T} \right)^2 \frac{e^{\hbar\omega/k_B T}}{(e^{\hbar\omega/k_B T} - 1)^2} \quad (\text{S.50})$$

When considering the limits to radiative heat transfer between metallic objects, one can expect that the resonances will have relatively small decay rates and thus that Φ will be very narrow, and much sharper than the Boltzmann-like distribution $f(\omega)$ in the integrand. Thus we approximate h by

$$h_{\text{rad}} \approx \frac{1}{A} k_B f(\omega_0) \int \Phi(\omega) d\omega. \quad (\text{S.51})$$

We take the metal to be a Drude metal with susceptibility $\chi(\omega) = -\omega_p^2/(\omega^2 + i\gamma\omega)$, for simplicity. Moreover, we assume that the absorption and emission of each body is described by a single sharp Lorentzian, with a narrow bandwidth (full-width at half-max) given by $\Delta\omega = \gamma$ [9, 10]. This is much narrower than e.g. the plane-plane and metamaterial structures in Fig. 3(a,b) and is in line with the resonant heat transfer between two spheres or between a sphere and a plate, depicted in Fig. 2 of the main text. The integral over Φ is approximately

$$\int \Phi(\omega) d\omega \approx \frac{\pi\gamma}{2} \Phi(\omega_0) \quad (\text{S.52})$$

and thus the radiative heat transfer coefficient is given by:

$$h_{\text{rad}} \approx \frac{1}{2} \pi \gamma k_B f(\omega_0) \frac{\Phi(\omega_0)}{A} \quad (\text{S.53})$$

The single-frequency limit to the flux per unit area is given by Eq. (6) in the main text, repeated here for a Drude metal:

$$\frac{\Phi(\omega_0)}{A} \leq \frac{1}{16\pi^2 d^2} \frac{\omega_p^4}{\gamma^2 \omega_0^2} \quad (\text{S.54})$$

Thus the limit to the radiative heat transfer coefficient is

$$h_{\text{rad}} \leq \frac{k_B \omega_0}{32\pi d^2} \frac{\omega_p^4}{\gamma \omega_0^3} f(\omega_0) \quad (\text{S.55})$$

From a design perspective, not each of the parameters in Eq. (10) is a free parameter. The choice of temperature, for

example, sets the optimal frequency (a blackbody at 300K has maximum emission at $7.6\mu\text{m}$ wavelength). Similarly, the factor ω_p/ω is limited by the optimal aspect ratio, and the factor γ/ω_p is set by the material loss rate. Hence, it is convenient to rewrite Eq. (10) as

$$h_{\text{rad}} \leq \frac{k_B^2 T}{\hbar} \left[\frac{1}{32\pi d^2} \frac{\omega_p^4}{\gamma \omega^3} g(\omega) \right] \quad (\text{S.56})$$

where $g = x^3 e^x / (e^x - 1)^2$ for $x = \hbar\omega/k_B T$.

The thermal conductivity of air is [11]:

$$\kappa_{\text{air}} = 0.026 \frac{\text{W}}{\text{m} \cdot \text{K}} \quad (\text{S.57})$$

Across a gap of size d , the conductive heat transfer coefficient is given by

$$h_{\text{cond}} = \frac{\kappa}{d} \quad (\text{S.58})$$

h_{rad} and h_{cond} are plotted in Fig. 3(c) in the main text for a variety of wavelengths and temperatures; also included are radiative heat transfer coefficients for plane-plane configurations, which fall short of the limits presented and require extremely small separation distances to even reach the conductive heat transfer coefficient.

-
- [1] Soumyadipta Basu and Mathieu Francoeur, “Maximum near-field radiative heat transfer between thin films,” *Applied Physics Letters* **98**, 243120 (2011).
 - [2] J. B. Pendry, “Radiative exchange of heat between nanostructures,” *Journal of Physics: Condensed Matter* **11**, 6621–6633 (1999).
 - [3] Philippe Ben-Abdallah and Karl Joulain, “Fundamental limits for noncontact transfers between two bodies,” *Physical Review B* **82**, 121419 (2010), arXiv:1009.4598.
 - [4] Svend-Age Biehs, “Radiative heat transfer between dielectric bodies,” (2011), arXiv:1103.3264.
 - [5] M. Cardona, “Fresnel Reflection and Surface Plasmons,” *American Journal of Physics* **39**, 1277 (1971).
 - [6] Stefan Alexander Maier, *Plasmonics: fundamentals and applications* (Springer Science & Business Media, 2007).
 - [7] S.-A. Biehs, M. Tschikin, and P. Ben-Abdallah, “Hyperbolic Metamaterials as an Analog of a Blackbody in the Near Field,” *Physical Review Letters* **109**, 104301 (2012).
 - [8] Jin Au Kong, *Theory of electromagnetic waves*, Vol. 1 (Wiley-Interscience, New York, NY, 1975).
 - [9] Feng Wang and Y. Ron Shen, “General Properties of Local Plasmons in Metal Nanostructures,” *Physical Review Letters* **97**, 206806 (2006).
 - [10] Aaswath Raman, Wonseok Shin, and Shanhui Fan, “Upper Bound on the Modal Material Loss Rate in Plasmonic and Metamaterial Systems,” *Physical Review Letters* **110**, 183901 (2013).
 - [11] William M Haynes, *CRC handbook of chemistry and physics* (CRC press, 2013).